Developmental Cell, Vol. 9, 489–499, October, 2005, Copyright ©2005 by Elsevier Inc. DOI 10.1016/j.devcel.2005.09.004

Cyclin D Regulation of a Sexually Dimorphic Asymmetric Cell Division

Christopher Tilmann[1,5,*] and Judith Kimble[1,2,3,4,*]
[1]Department of Biochemistry
[2]Department of Genetics
[3]Laboratory of Molecular Biology
[4]Howard Hughes Medical Institute
University of Wisconsin-Madison
433 Babcock Drive
Madison, Wisconsin 53706

Summary

The *C. elegans* somatic gonadal precursor cell (SGP) divides asymmetrically to establish gonad-specific coordinates in both sexes. In addition, the SGP division is sexually dimorphic and initiates sex-specific programs of gonadogenesis. Wnt/MAPK signaling determines the gonadal axes, and the FKH-6 transcription factor specifies the male mode of SGP division. In this paper, we demonstrate that *C. elegans* cyclin D controls POP-1/TCF asymmetry in the SGP daughters as well as *fkh-6* and *rnr* expression in the SGPs. Although cyclin D mutants have delayed SGP divisions, the cyclin D defects are not mimicked by other methods of retarding the SGP division. We find that EFL-1/E2F has an antagonistic effect on *fkh-6* expression and gonadogenesis, which is relieved by cyclin D activity. We propose that cyclin D and other canonical regulators of the G1/S transition coordinate key regulators of axis formation and sex determination with cell cycle progression to achieve the sexually dimorphic SGP asymmetric division.

Introduction

Asymmetric cell divisions are a widespread mechanism for generating diverse cell types during animal development (Betschinger and Knoblich, 2004). Model asymmetric divisions include those of the *C. elegans* zygote, the *C. elegans* EMS blastomere, and the *Drosophila* neuroblast and sensory organ precursor (Ahringer, 2003; Bei et al., 2002; Cowan and Hyman, 2004; Doe and Bowerman, 2001; Roegiers and Jan, 2004). We have embarked on an in depth analysis of a different asymmetric division, that of the somatic gonadal precursor cell (SGP) in *C. elegans*. This division establishes the proximal-distal axis of the gonad of both sexes, and it is sexually dimorphic (Kimble and Hirsh, 1979). By teasing apart the molecular regulators of the SGP division, we will learn how precursor cells establish an organ coordinate system and how asymmetric divisions can be modulated during development to generate distinct organs.

The *C. elegans* embryo generates a four-celled gonadal primordium that appears the same in XX hermaphrodites and XO males (Kimble and Hirsh, 1979; Mathies et al., 2004; Sulston et al., 1983). Within the primordium, one SGP resides at each of the two opposite poles, and two germline precursors lie between (Figure 1A). During the first larval stage (L1), the SGP divides asymmetrically in both sexes to generate proximal and distal daughters that establish gonadal axes. The SGP division is also sexually dimorphic with respect to both size and fate of its daughters. The hermaphrodite SGP makes distal and proximal daughters of roughly equal size, but the male SGP produces a smaller distal daughter and a larger proximal daughter (Figure 1A). In addition, the SGP daughters exhibit sex-specific behaviors (e.g., migration) (Figure 1A) and generate sex-specific regulatory cells that control gonad elongation and germline proliferation (Figure 1B). Therefore, the SGP asymmetric division initiates sex-specific programs of gonadogenesis that generate a double-armed ovotestis in hermaphrodites and a single-armed testis in males (Figure 1B).

Two major pathways of regulation converge to regulate the SGP division. The first is gender neutral: the Wnt/MAPK pathway specifies the distal SGP daughter fate in both sexes (Kidd et al., 2005; Siegfried and Kimble, 2002; Siegfried et al., 2004; Sternberg and Horvitz, 1988). The terminal regulators of this pathway are POP-1/TCF and SYS-1/β-catenin, a DNA binding protein and its transcriptional coactivator, respectively (Kidd et al., 2005; Lin et al., 1995). In the early embryo, activated Wnt/MAPK signaling promotes nuclear export of POP-1 so that the daughter cell receiving the Wnt signal has less nuclear POP-1 than its sister, a phenomenon called POP-1 asymmetry (Lo et al., 2004; Maduro et al., 2002). A similar situation is observed after the SGP division: the distal daughter is specified by Wnt/MAPK activation and contains less nuclear POP-1 than its proximal sister (Siegfried et al., 2004). In mutants lacking POP-1, SYS-1, or upstream components of the Wnt/MAPK pathway, distal-specific cells are not made, and extra proximal-specific cells are sometimes seen (Miskowski et al., 2001; Siegfried and Kimble, 2002; Siegfried et al., 2004; Sternberg and Horvitz, 1988); by contrast, gonads with excess SYS-1 produce extra distal cells and lack proximal cells (Kidd et al., 2005). Therefore, the Wnt/MAPK pathway establishes the proximal-distal axes of both hermaphrodite and male gonads.

The second pathway controls the sexual dimorphism of the SGP division. Most important for this work are two transcription factors. FKH-6 is a forkhead transcription factor that specifies the male-specific SGP division during the first larval stage of development (Chang et al., 2004). FKH-6 controls sex determination, specifically in the SGPs, and does not affect sex determination in other tissues or at other times of gonadal development; however, it does have a second and more poorly defined late larval role in hermaphrodite gonadogenesis (Chang et al., 2004). TRA-1 is the *C. elegans* GLI transcription factor that acts in virtually all tissues to specify the female fate (Hodgkin and Brenner, 1977;

*Correspondence: jekimble@wisc.edu (J.K.); cetilmann@loyola.edu (C.T.)
[5]Present address: Department of Biology, Loyola College in Maryland, 4501 North Charles Street, Baltimore, Maryland 21210.

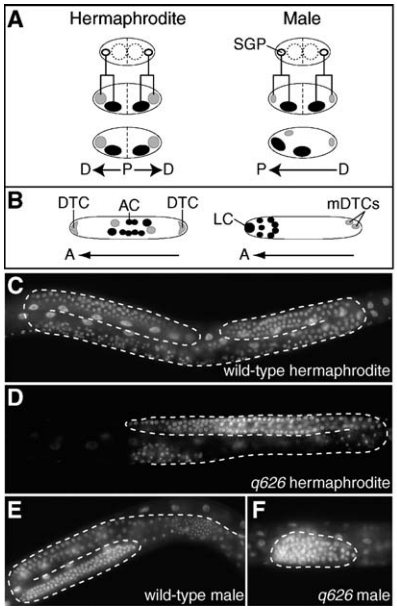

G Hermaphrodite

Genotype	°C	Number of gonadal arms (%) Two	One	None	n
wild-type	20 or 25	100	0	0	123
q626	20	100	0	0	99
q626	25	60	38	2	82

H Male

Genotype*	°C	Gonad morphology (%) Extended	Disorgan.	n
wild-type	20/25	100	0	134
q626	20	97	3	105
q626	25	18	82	145

*all strains carry *him-5(e1490)* to generate males.

I Hermaphrodite

Time at 25°C	Number of gonadal arms (%) Two	One	None	n
L1 molt to adult	100	0	0	62
hatching to L1 molt	82	16	2	76

J Male

Time at 25°C	Gonad morphology (%) Extended	Disorgan.	n
hatching to adult	37	63	64
L1 molt to adult	100	0	89
hatching to L1 molt	28	72	53

Figure 1. The *q626* Mutation Affects Hermaphrodite and Male Gonadogenesis

(A) Early events in hermaphrodite and male gonadogenesis. Top diagrams: four-celled gonadal primordium. SGPs, open circles; germline precursors, dashed circles. Middle diagrams: the SGPs divide asymmetrically to produce proximal (dark) and distal (light) daughters. Hermaphrodite proximal and distal daughters are of roughly equal size and do not migrate, creating two proximal-distal (P-D) axes. Male proximal daughters are larger than their distal sisters, and they migrate anteriorly to create a single P-D axis.

(B) Gonadal regulatory cells in the L2/L3 developing somatic gonad. Left, hermaphrodite; right, male. Cells derived from the distal SGP daughter, light gray; cells derived from the proximal SGP daughter, dark gray. A, Anterior. In hermaphrodites, the distal tip cells (DTCs) control both arm elongation and germline proliferation, and the anchor cell (AC) induces vulval development. In males, the linker cell (LC) controls elongation of the single gonadal arm, and male distal tip cells (mDTCs) control germline proliferation.

(C–F) DAPI-stained L4s grown at 25°C. Dashed line, boundaries of gonadal tissue. (C) Wild-type hermaphrodite gonad with two U-shaped gonad arms. (D) *q626* hermaphrodite gonad with one gonad arm. (E) Wild-type male with one J-shaped gonad arm. (F) *q626* male with nonextended, disorganized gonad.

(G–J) Tables quantifying the penetrance of gonadal defects. Disorgan., disorganized. (I–J) Temperature shift experiments with *q626* mutants.

Mathies et al., 2004; Zarkower and Hodgkin, 1992). The XO gonad is feminized and disorganized in *fkh-6* null mutants, and the XX gonad is masculinized in *tra-1* null mutants (Hodgkin and Brenner, 1977; Mathies et al., 2004). The SGP division in *fkh-6; tra-1* double mutants is hermaphrodite-like, indicating that TRA-1 acts upstream of FKH-6 (Chang et al., 2004). Therefore, FKH-6 is the terminal regulator of the SGP male fate.

In this paper, we identify the single *C. elegans* cyclin D gene, *cyd-1*, as a key regulator of axis formation and sex determination in the gonad. Cyclin D functions during L1, and it appears to be specific to the SGP and its immediate daughters. The *cyd-1(q626)* mutation is a missense allele, and its effects can be mimicked by *cyd-1* RNAi. Cyclin D has its effect on gonadogenesis via the canonical cell cycle machinery, including the cyclin-dependent kinase 4 (*cdk-4*), Rb (*lin-35*), E2F (*efl-1*), DP (*dpl-1*), the CDK inhibitors (*cki-1* and *cki-2*), and cyclin E (*cye-1*). Cyclin D affects axis determination in both sexes by promoting POP-1 asymmetry and controls the sex-specific cell size asymmetry of the male SGP division, apparently by relieving E2F repression of the *fkh-6* gonad-specific sex determination gene. Cyclin D also affects *rnr::GFP* expression, specifically in SGPs, and slows the SGP cell cycle. However, other methods of slowing the SGP cell cycle did not mimic *cyd-1* defects. We propose that cyclin D and regulators of the G1/S transition coordinate both specification of distal-proximal organ axes and specification of sexual fate with the cell cycle.

Results

Early Gonadogenesis Defects in *q626* Mutants

We have isolated a temperature-sensitive mutation, called *q626* (see Experimental Procedures). At the permissive temperature of 20°C, *q626* homozygotes of either sex were virtually normal, but, at the restrictive temperature of 25°C, they had gonadal defects in both sexes. Normally, hermaphrodites have a gonad with two extended U-shaped "arms," one anterior and one posterior (Figures 1C and 1G), but when raised at 25°C, some *q626* hermaphrodites were missing either one or both arms (Figures 1D and 1G). Importantly, *q626* hermaphrodites with one gonadal arm were self-fertile, and no other gonadal defects were observed. In contrast to this relatively mild effect on hermaphrodites, *q626* had a severe effect on male gonadogenesis. Wild-type adult males and most adult *q626* males raised at 20°C have an extended J-shaped gonad (Figures 1E and 1H). By contrast, most adult *q626* males had disorganized gonads that were not extended when raised at 25°C (Figures 1F and 1H). Furthermore, some male *q626* mutants developed a hermaphrodite vulva (3%, n = 145; data not shown). These *q626* effects were gonad specific in both sexes: growth was similar to that of wild-type animals, movement seemed unaffected, nongonadal tissues developed normally, and embryonic survival was normal.

To learn when *q626* affects gonadogenesis, we imposed selected temperature regimens on this temperature-sensitive mutant. In both hermaphrodites and males, the gonad developed normally when raised at the permissive temperature during the L1 stage and then shifted to the restrictive temperature from the L1 molt through adulthood; by contrast, gonad development was defective when L1 larvae were exposed to the restrictive temperature and were then returned to the permissive temperature from the L1 molt through adulthood (Figures 1I and 1J). We conclude that *q626* affects gonadogenesis during the L1 stage in both sexes.

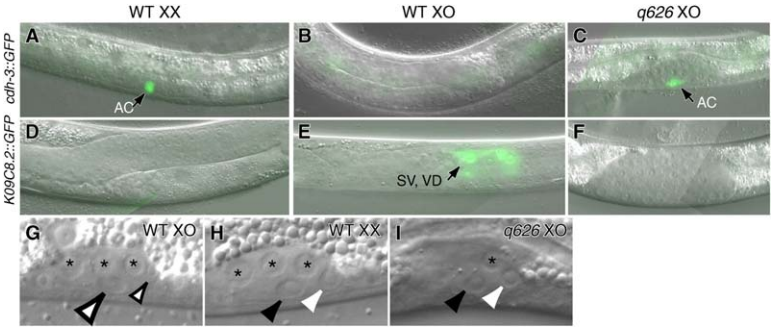

Figure 2. *q626* Feminizes the Gonad and Appears to Function Like *fkh-6*

(A–C) L3 animals carrying anchor cell (AC) marker, *cdh-3::GFP*. (A) Wild-type hermaphrodite. (B) Wild-type male. (C) *q626* male raised at the restrictive temperature expresses the AC marker.

(D–F) L4 animals carrying marker for vas deferens (VD) and seminal vesicle (SV), *K09C8.2::GFP*. (D) Wild-type hermaphrodite. (E) Wild-type male. (F) *q626* male raised at the restrictive temperature does not express the SV/VD marker.

(G–I) L1 gonads viewed by Nomarski microscopy. Asterisks, germ cells. (G) Male SGP daughters differ in size. Small, open arrow, smaller distal daughter; large, open arrow, larger proximal daughter. (H) Hermaphrodite SGP daughters are of roughly equal size. White arrowhead, distal daughter; black arrowhead, proximal daughter. (I) *q626* SGP daughters at the restrictive temperature are of roughly equal size. Same conventions as (H).

q626 Affects Generation of Regulatory Cells in Both Sexes

Normally, the SGP division generates distal and proximal daughter cells that generate regulatory cells critical for gonad shape and germline proliferation in both sexes (Kimble, 1981; Kimble and White, 1981). Gonadal arm elongation is controlled by "leader cells," which are distal tip cells (DTCs) in hermaphrodites and the linker cell (LC) in males (Kimble and White, 1981). Leader cells express *lag-2::GFP* brightly (Blelloch et al., 1999). At the restrictive temperature, about one-third of *q626* hermaphrodites were missing one *lag-2::GFP*-expressing DTC (32%, n = 91, data not shown), and about one-half of *q626* males were missing the *lag-2::GFP*-expressing LC (58%, n = 78, data not shown). Therefore, the lack of arm extension in *q626* gonads is due to missing leader cells.

The size of *q626* male gonads was variable, apparently due to a varying extent of germline proliferation. In males, germline proliferation is controlled by "male DTCs" (mDTCs), two small cells residing near the distal tip of the wild-type male gonad (Kimble and White, 1981). These mDTCs also express *lag-2::GFP*, but that expression is much weaker than in leader cells (Blelloch et al., 1999). Whereas all wild-type male gonads had two *lag-2::GFP*-expressing mDTCs (100%, n = 20), only a small percentage of *q626* males had detectable *lag-2::GFP*-expressing mDTCs (23%, n = 78). Therefore, mDTCs are not generated normally in *q626* XO gonads. We conclude that *q626* affects the production of distal SGP daughters in both sexes.

q626 Feminizes the XO Gonad

The *q626* male gonadal defects were reminiscent of *fkh-6* XO gonads, which are disorganized, lack linker cells, and sometimes induce vulvae (Chang et al., 2004). Because male *fkh-6* gonads are also feminized (or perhaps more correctly hermaphroditized) (Chang et al., 2004), we examined *q626* gonads with markers for hermaphrodite and male gonadal differentiation. The hermaphrodite-specific marker *cdh-3::GFP* labels the hermaphrodite anchor cell, but it is not expressed in wild-type male gonads (Figures 2A and 2B) (Pettitt et al., 1996); however, *cdh-3::GFP* expression occurred in most *q626* males (67%, n = 15; Figure 2C). By contrast, the male-specific marker *K09C8.2::GFP* labels the male seminal vesicle and vas deferens, but it is not expressed in wild-type hermaphrodite gonads (Figures 2D and 2E) (Chang et al., 2004); *K09C8.2::GFP* was not detected in some *q626* males (45%, n = 51; Figure 2F). Finally, three other hermaphrodite-specific markers of gonadal differentiation were expressed in most *q626* male gonads: *lim-7::GFP* (sheath cells), *fkh-6::GFP* (sheath and spermatheca), and *ZK813.3::GFP* (spermatheca) (data not shown). We conclude that the disorganized gonads in *q626* males are feminized.

We next asked if the SGP asymmetric division and the behavior of SGP daughter cells were feminized in *q626* males. Hermaphrodite SGPs produce daughters of approximately equal size (Figures 1A and 2H), and their proximal daughters do not migrate; however, male SGPs produce daughters of unequal size (Figures 1A and 2G), and their proximal daughters migrate toward the anterior. In *q626* males, the SGP daughters were of roughly equal size (Figure 2I), and most proximal daughters did not migrate (92%, n = 13). We conclude that *q626* feminizes both the SGP asymmetric division and later gonadal differentiation.

q626 Is a *cyd-1* Missense Mutation

We cloned the gene corresponding to *q626* by standard methods (see Experimental Procedures). Three lines of evidence showed that *q626* is an allele of *cyd-1,* which encodes the single *C. elegans* homolog of cyclin D1 (Boxem and van den Heuvel, 2001; Park and Krause, 1999). First, the *cyd-1(q626)* genomic sequence revealed a missense mutation just C-terminal to the cyclin box in a region conserved between closely related nematodes, but not in vertebrates (Figures 3A and 3B). Second, a DNA fragment spanning the *cyd-1* locus was able to rescue *q626* gonadal defects (see Experimental Procedures). Finally, *q626* failed to complement either of two *cyd-1* null mutations (*he112* and *he116*).

We next asked if *cyd-1(q626)* alters gonad-specific activity or reduces activity more generally. The *cyd-1(he116)* allele, henceforth called *cyd-1(0)*, deletes the promoter region and the first two exons and is thought to be a null allele (Boxem and van den Heuvel, 2001). Most postembryonic divisions are blocked in *cyd-1(0)* mutants, but the SGP division is an exception (Koreth

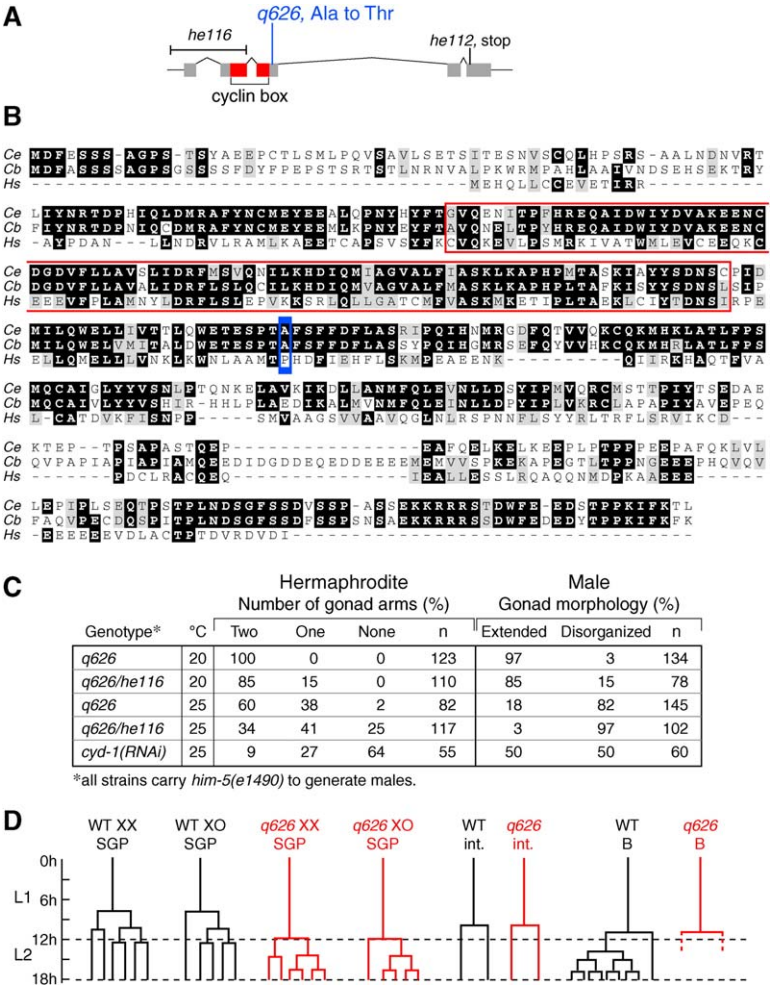

Figure 3. *q626*, a Missense Mutation in *cyd-1* that Delays SGP Division

(A) The *cyd-1* gene. Boxes, exons; lines, introns; red, cyclin box. *q626* is a G-to-A base change that generates a missense mutation predicted to change an alanine to threonine. *he116* and *he112* are both predicted *cyd-1* null mutations (Boxem and van den Heuvel, 2001).

(B) Alignment of *C. elegans* (top), *C. briggsae* (middle), and human cyclin D1 (bottom) amino acid sequences (black boxes, identical residues; gray boxes, similar residues). The *q626* mutation (blue box) is in a conserved region that lies to the C-terminal side of the cyclin box (red outline).

(C) Gonad defects typical of *cyd-1(q626)* are more severe when placed over *cyd-1(0)* and are observed after depletion of *cyd-1* by RNAi.

(D) Comparison of cell divisions in wild-type (WT, black) and *cyd-1(q626)* mutants raised at the restrictive temperature (red). L1, first larval stage; L2, second larval stage. Time scale in hours at 25°C. SGP divisions are delayed in *cyd-1(q626)* mutants relative to wild-type, but other blast cell divisions are normal.

and van den Heuvel, 2005). We confirmed that *cyd-1(0)* SGPs divide once or, at most, twice, and that gonadal development then arrests in both sexes. Indeed, although later gonadal development did not occur in *cyd-1* null mutants, the male SGPs generated daughters of roughly equal size, and proximal SGP daughters did not migrate. Both of these findings are diagnostic of a feminized SGP division (n = 6). To assay later gonadal development, we turned to *cyd-1(q626)/cyd-1(0)* transheterozygotes and *cyd-1* RNAi. Gonadal defects were more penetrant in *cyd-1(q626)/cyd-1(0)* transheterozygotes than in *cyd-1(q626)* homozygotes, at both permissive and restrictive temperatures and in both sexes (Figure 3C). Furthermore, *cyd-1* RNAi gonads were affected much like *cyd-1(q626)* (Figure 3C). The simplest explanation is that the *cyd-1(q626)* lesion reduces activity of the locus.

SGP Divisions Are Delayed in *cyd-1* Males and Hermaphrodites

We next asked if the timing of cell divisions was impaired in *cyd-1(q626)* mutants relative to wild-type. At the restrictive temperature, wild-type SGPs divided between 7 and 9 hr after hatching in both sexes (males, n = 9; hermaphrodites, n = 13), and two subsequent divisions in the SGP lineage occurred at approximately 10 and 13 hr after hatching, respectively (Figure 3D). By contrast, *cyd-1(q626)* SGPs divided 12 or more hr after hatching, just prior to or during the L1 molt, in both sexes (males, n = 7; hermaphrodites, n = 11) (Figure 3D). Subsequent rounds of division occurred during L2, and their timing was normal relative to the SGP division (Figure 3D). Intestinal divisions were not delayed in *cyd-1(q626)* mutants, and the adult number of intestinal nuclei was normal (n = 20; Figure 3D). Similarly, the B blast cell divided normally in *cyd-1(q626)* males (n = 20; Figure 3D), and both *cyd-1(q626)* hermaphrodites and males had the normal number of coelomocytes (six in hermaphrodites, five in males), which was seen when using the *unc-122::GFP* coelomocyte marker (data not shown). Therefore, *cyd-1(q626)* SGP divisions are delayed specifically, but that delay is not sexually dimorphic.

Control of Gonadogenesis by Other Cell Cycle Regulators

We next investigated other components of the cell cycle machinery for effects on gonadogenesis (Figure 4A). To learn whether CYD-1 works with its CDK-4 partner to control gonadogenesis, we depleted *cdk-4* during

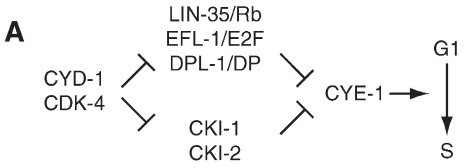

B

Genotype	°C	Male gonad: Disorg (%)	Male gonad: Fem (%)	Male gonad: n	Herm. gonad: One arm (%)	Herm. gonad: No arms (%)	Herm. gonad: n
cyd-1	20	3	N	105	0	0	99
cyd-1	25	82	Y	145	38	2	82
cdk-4(RNAi)	20	0	N	36	10	0	22
cyd-1; cdk-4(RNAi)	20	89	Y	70	18	73	55
cye-1(RNAi)	20	5	N	42	2	0	48
cyd-1; cye-1(RNAi)	20	39	Y	66	23	38	52
lin-35; cyd-1	25	4	ND	54	0	0	97
cyd-1; efl-1(RNAi)	25	11	ND	70	2	0	92
cyd-1; dpl-1(RNAi)	25	21	ND	48	12	0	66
cyd-1; cki-1(RNAi)	25	49	ND	55	19	0	67
cyd-1; cki-2(RNAi)	25	64	ND	64	27	3	67
cyd-1; cki-1&-2(RNAi)	25	27	ND	66	16	0	52
HU treatment	20	0	ND	37	0	0	80

Figure 4. Regulators of the G1/S Transition Enhance or Suppress *cyd-1* Gonad Defects

(A) Diagram of G1/S regulators relevant to this work, and their functional relationships. CYD-1, cyclin D; CDK-4, cyclin-dependent kinase; LIN-35/Rb, *C. elegans* homolog of the human retinoblastoma gene; EFL-1, *C. elegans* homolog of E2F; DPL-1, *C. elegans* homolog of DP; CKI, inhibitors of CDK; see Koreth and van den Heuvel (2005) for review.

(B) Effects of cell cycle regulators on gonadogenesis. RNAi, RNA-mediated interference. HU, hydroxyurea; Disorg, disorganized; Fem, feminized as assessed by using three hermaphrodite-specific gonad markers.

larval development by using RNAi, but *cdk-4(RNAi)* effects were minimal (Figure 4B). Nonetheless, *cdk-4(RNAi)* enhanced *cyd-1(q626)* gonadogenesis defects: at the permissive temperature (20°C), *cyd-1(q626); cdk-4(RNAi)* hermaphrodite gonads had missing arms and *cyd-1(q626); cdk-4(RNAi)* male gonads were misshapen (Figure 4B). Most importantly, the *cyd-1(q626); cdk-4(RNAi)* male gonads expressed hermaphrodite-specific gonadal markers for anchor cell, sheath, and spermatheca (60%, n = 33). Therefore, *cyd-1* and *cdk-4* are likely to work together to control gonadal sex determination.

CYD-1/CDK-4 promotes S phase initiation by inhibiting two parallel sets of regulators (Koreth and van den Heuvel, 2005) (Figure 4A). The first set includes LIN-35/Rb, EFL-1,2/E2F, and DPL-1/DP, and the second includes two inhibitors, CKI-1 and CKI-2 (Koreth and van den Heuvel, 2005). We therefore asked if *cyd-1* defects could be suppressed by removal or depletion of these downstream genes. Our results are summarized in Figure 4B. Briefly, *cyd-1* defects were suppressed by *lin-35(0)*, *efl-1(RNAi)*, *dpl-1(RNAi)*, and *cki-1/cki-2(RNAi)*: XO gonads were fully male, and XX gonads had two arms and were self-fertile. Therefore, *cyd-1* appears to be acting through *lin-35*, *efl-1*, *dpl-1*, and the *cki* genes to control the SGP division.

C. elegans cyclin E is encoded by a single gene, *cye-1*, which acts downstream of *cyd-1* to control entry into S phase (Koreth and van den Heuvel, 2005) (Figure 4A). Although *cye-1(RNAi)* male and hermaphrodite gonads were largely normal, *cye-1(RNAi)* enhanced the *cyd-1(q626)* defects at the permissive temperature: *cyd-1(q626); cye-1(RNAi)* animals of both sexes had defective gonads (Figure 4B), and male gonads expressed hermaphrodite-specific gonadal markers (56%, n = 25). Therefore, *cye-1* appears to affect the SGP division in the same manner as *cyd-1*. The simplest interpretation is that *cyd-1* affects gonadogenesis through the canonical cell machinery that controls the G1/S phase transition.

Slowing the SGP Cell Cycle Does Not Mimic *cyd-1(q626)* Defects

Previous studies have shown that a delayed cell cycle can nonspecifically alter cell fate decisions or asymmetric divisions (Ambros, 1999; Encalada et al., 2000; Tio et al., 2001). To ask if SGP defects typical of *cyd-1(q626)* were induced by a lengthened S phase, we treated L1s with hydroxyurea (HU) prior to the SGP division to slow S phase. HU treatment did indeed delay the SGP division by 4 or more hr, but no gonad defects were observed in either sex (Figure 4B). To ask if these SGP defects might be induced by a delay in SGP divisions relative to other cells in the animal, we employed *gon-4* RNAi. Previous work showed that SGP divisions are retarded specifically in *gon-4* null mutants; other cell divisions were not delayed (Friedman et al., 2000). Using *gon-4* RNAi, we found the same effect: most SGP divisions were delayed by ~3 hr, but others (e.g., B, I) were not. We focused on the delayed SGP divisions: hermaphrodite SGPs generated roughly equal-sized daughters that did not migrate (n = 14), and male SGPs generated dramatically larger proximal daughters that moved anteriorly (n = 8). Therefore, it seems unlikely that an SGP-specific cell cycle delay is responsible for the aberrant SGP divisions in *cyd-1* mutants.

cyd-1 Promotes POP-1/TCF Asymmetry in SGP Daughters

The POP-1 and SYS-1 transcription factors control the generation of SGP daughters with distal fates in both sexes (see Introduction). Because distal cells are often missing in *cyd-1(q626)* mutants, we reasoned that *cyd-1(q626)* might affect the Wnt/MAPK pathway. Loss-of-function *sys-1* mutations are haploinsufficient and dominantly enhance mutations in other Wnt/MAPK components, while ectopic *sys-1* expression can reverse SGP daughter fates and suppress mutations in upstream Wnt/MAPK components (Kidd et al., 2005; Siegfried et al., 2004). We found that a *sys-1* loss-of-function mutation is similarly a strong dominant enhancer of *cyd-1(q626)* at both the permissive and restrictive temperatures, and that ectopic SYS-1 can suppress *cyd-1(q626)* (Figure 5A). Therefore, *cyd-1(q626)* appears to influence the Wnt/MAPK pathway.

We next asked if *cyd-1(q626)* affects POP-1 asymmetry. In wild-type animals, GFP::POP-1 is higher in the nuclei of proximal than distal SGP daughters (Figures 6B–6D; Siegfried et al., 2004). By contrast, in *cyd-1(q626)* hermaphrodites, GFP::POP-1 asymmetry in SGP daughters was sometimes abolished: in 4 of 12 animals,

A

Genotype*	°C	Hermaphrodite Number of gonad arms (%) Two	One	None	n
cyd-1	20	100	0	0	99
sys-1/+	20	94	6	0	>100
sys-1/+; cyd-1	20	30	40	30	46
cyd-1	25	60	38	2	82
sys-1/+	25	94	6	0	>100
sys-1/+; cyd-1	25	0	0	100	49
cyd-1; hs::sys-1	25	80	20	0	120

*cyd-1=q626; sys-1=q736

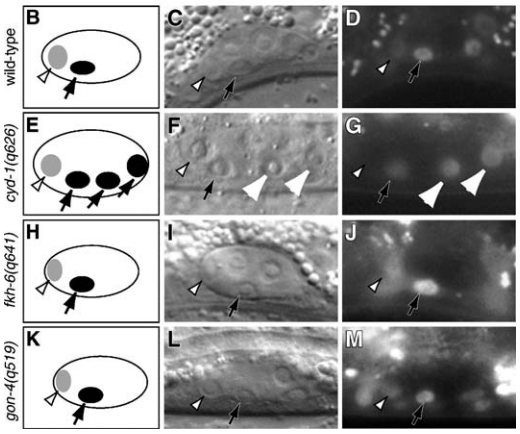

Figure 5. POP-1 Asymmetry in SGP Daughters Can Be Abolished in *cyd-1* Mutants

(A) Genetic interactions between *cyd-1* and *sys-1*.

(B–J) Left column, diagrams showing POP-1 abundance in SGP daughters. Light gray, low POP-1; dark gray, high POP-1. Middle column: Nomarski micrographs of SGP daughters. Open arrowhead, distal sister with less POP-1; solid arrow, proximal sister with more POP-1; white arrowheads, sisters with equal amounts of POP-1. Right column: same gonads as in the middle column, showing fluorescence of the GFP::POP-1 reporter. All gonads shown are from XX hermaphrodites. (B–D) Wild-type gonad. GFP::POP-1 is localized asymmetrically in SGP daughters. (E–G) *cyd-1(q626)* gonad. GFP::POP-1 is localized asymmetrically in anterior SGP daughters (left) and equally in posterior SGP daughters (right). (H–J) *fkh-6* null mutant gonad. GFP::POP-1 is localized asymmetrically in SGP daughters.

(K–M) *gon-4(RNAi)* gonad. GFP::POP-1 is localized asymmetrically in SGP daughters.

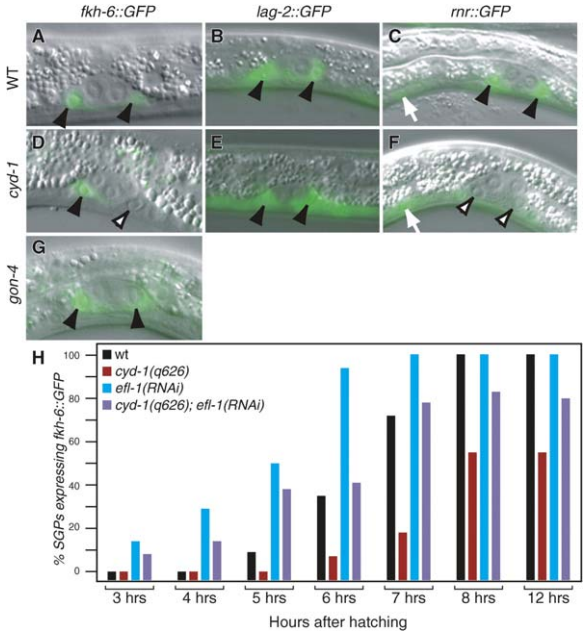

Figure 6. Gene Expression in *cyd-1(q626)* Mutants

(A–H) (A–C) Wild-type L1 larvae raised at 25°C; (D–F) *cyd-1(q626)* L1 larvae raised at 25°C. Solid arrow, SGPs expressing marker; open arrowheads, SGPs that do not express marker; white arrow, nongonadal cell-expressing marker. All images are XX larvae, but the same results are seen in XO larvae. (A–C) Wild-type SGPs express (A) *fkh-6::GFP*, (B) *lag-2::GFP*, and (C) *rnr::GFP*. (D) Some *cyd-1(q626)* SGPs express *fkh-6::GFP* (arrow), and others do not (open arrowhead). (E) All *cyd-1(q626)* SGPs express *lag-2::GFP*. (F) Most *cyd-1(q626)* SGPs do not express *rnr::GFP* (open arrowheads), but nongonadal cells express *rnr::GFP* normally (large arrowhead). (G) *gon-4(RNAi)* gonads express *fkh-6::GFP*. (H) Time course of *fkh-6::GFP* expression in WT (black), *cyd-1(q626)* (red), *elf-1(RNAi)* (blue), and *cyd-1(q626); efl-1(RNAi)* (purple) gonads.

nuclear GFP::POP-1 was present at approximately equal levels in one pair of SGP daughter cells (Figures 5E–5G). The frequency of this defect in POP-1 asymmetry was similar to that at which *cyd-1(q626)* hermaphrodites are missing a gonadal arm. We also examined GFP::POP-1 in *fkh-6(0)* hermaphrodites, which sometimes lack a DTC (Chang et al., 2004), but we found no effect on GFP::POP-1 asymmetry (n = 67; Figures 5H–5J). GFP::POP-1 localization was also not affected by *gon-4(RNAi)* (Figures 5K–5M). Therefore, *cyd-1*, but not *fkh-6* or *gon-4*, influences POP-1 asymmetry in SGP daughters.

To find out if *cyd-1(q626)* affects POP-1 asymmetry in nongonadal tissues, we examined T cell and V cell daughters. In wild-type hermaphrodites, nuclear GFP::POP-1 is more abundant in anterior T and V daughters (Herman, 2002). Similarly, POP-1 asymmetry was normal in T and V cell daughters in *cyd-1(q626)* mutants (n = 28). We also looked for T cell lineage defects in *cyd-1(q626)* animals by their ability to take up the lipophilic dye, DiO (Herman and Horvitz, 1994). In wild-type animals, descendents of the T cell (phasmid neurons in the tail, PHA and PHB) stain with this dye. DiO was taken up normally by phasmid neurons in all *cyd-1(q626)* mutants (n = 84). We conclude that the *cyd-1(q626)* defect in POP-1 asymmetry is specific to the SGPs.

cyd-1 Controls *fkh-6* Expression in the SGPs

The similarity of the *cyd-1(q626)* and *fkh-6* gonadal defects suggested that *cyd-1* might control *fkh-6* expression. In wild-type animals, a *fkh-6::GFP* reporter is expressed in the SGPs of both sexes beginning in L1, prior to the first SGP division. In hermaphrodites, *fkh-6::GFP* expression ceases just after the SGP division, but, in males, expression persists several hours after the SGP division. *fkh-6::GFP* is also expressed much later (L3 to adult) in the hermaphrodite spermatheca (Chang et al., 2004). In wild-type animals of both sexes, *fkh-6::GFP* expression began in the SGPs at about 6 hr after hatching (Figures 6A and 6H, black bars). By contrast, *fkh-6::GFP* expression was either delayed or absent in the SGPs of *cyd-1(q626)* mutants in both

sexes (Figures 6D and 6H, red bars). Specifically, few SGPs expressed *fkh-6::GFP* 6 hr after hatching, only about half expressed the reporter after 8 hr (males, 50%, n = 60; hermaphrodites, 43%, n = 124), and even 12 hr after hatching, *fkh-6::GFP* was absent from many SGPs (Figures 6D and 6H, red bars). In those *cyd-1(q626)* mutants that did express *fkh-6::GFP*, that expression ceased as normal in both hermaphrodites (just after the SGP division) and males (several hours after the SGP division). Therefore, *cyd-1* does not affect the sexually dimorphic nature of *fkh-6* expression. Furthermore, *fkh-6::GFP* was not seen in *cyd-1(0)* SGPs (n = 38 SGPs, data not shown). The hermaphrodite spermathecal expression could not be tested in *cyd-1(0)* mutants, but it appeared normal in *cyd-1(q626)* hermaphrodites at the restrictive temperature (100%, n = 50). We also examined *fkh-6::GFP* expression in *gon-4(RNAi)* animals and *gon-4(q519)* mutants and found no defects (n = 26, Figure 6G). Therefore, *cyd-1* controls *fkh-6* expression specifically in the SGPs of both sexes.

We next examined other SGP markers. In wild-type larvae, *tra-1::GFP*, *pes-1::GFP*, and *lag-2::GFP* are all expressed in both hermaphrodite and male SGPs (Hope, 1991; Mathies et al., 2004) (Figure 6B, data not shown); similarly, all three reporters were expressed in SGPs of both *cyd-1(q626)* and *cyd-1(he116)* mutants in both sexes (Figure 6E; data not shown). Therefore, *cyd-1* does not control gene expression in SGPs generally. Finally, we looked at the *rnr::GFP* S phase marker (Hong et al., 1998). In wild-type L1 larvae, *rnr::GFP* expression first begins in the SGPs approximately 6 hr after hatching, and also occurs in other dividing cells (Figure 6C). By contrast, *rnr::GFP* was rarely expressed in *cyd-1(q626)* SGPs (6%, n = 32 SGPs), but it was expressed in nongonadal cells (Figure 6F). We conclude that *cyd-1* affects the expression of both *fkh-6::GFP* and *rnr::GFP* expression specifically in the SGPs.

Cyclin D Appears to Relieve E2F Repression of *fkh-6::GFP*

Cyclin D functions, at least in part, to relieve E2F repression of target genes during the G1/S transition (Coffman, 2004; Koreth and van den Heuvel, 2005). We therefore considered the idea that the *efl-1/E2F* gene might repress *fkh-6* expression. Consistent with that possibility, we sought potential E2F binding sites in the 5′ flanking region of *fkh-6*, and we found one possibility (TTTGCGG) at positions –1584 to –1577. As described above, *fkh-6::GFP* expression in SGPs is delayed or absent in *cyd-1* mutants of both sexes compared to wild-type. In *efl-1* RNAi animals, *fkh-6::GFP* was expressed, and it was in fact expressed earlier than in wild-type (Figure 6H, blue bars). Although expression of *fkh-6::GFP* occurred earlier than normal in both hermaphrodites and males, hermaphrodite gonadogenesis remained normal and was not masculinized; male gonadogenesis was also normal and not feminized. Earlier expression of *fkh-6::GFP* was also seen in *cyd-1(q626); efl-1(RNAi)* SGPs (Figure 6H, purple bars). Therefore, *fkh-6::GFP* expression appears to be repressed by E2F, and cyclin D appears to relieve that repression.

A

	Male Gonad morphology (%)				Hermaphrodite Number of gonad arms (%)			
Genotype	Extended	Disorg.	Arrest	n	Two	One	None	n
fkh-6	0	100	0	>100	91	9	0	>100
tra-1	82	18	0	>100	NA	NA	NA	–
cyd-1	18	82	0	>100	60	38	2	82
fkh-6 cyd-1	0	100	0	70	17	37	46	70
fkh-6; tra-1	0	10	90	42	NA	NA	NA	–
cyd-1; tra-1	0	60	40	87	NA	NA	NA	–

B

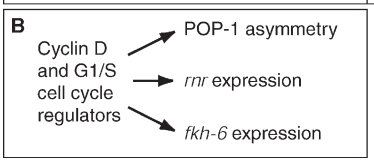

Figure 7. Cyclin D Coordinates Key Regulators of the SGP Asymmetric Division

(A) Table comparing effects of *cyd-1(q626)* and *fkh-6(0)* mutations on gonadogenesis as single or double mutants.
(B) See text for explanation.

Functional Relationship of *cyd-1* and *fkh-6*

Loss-of-function mutations in *cyd-1* and *fkh-6* have similar effects on gonadal sex determination (this work; Chang et al., 2004), and *fkh-6* expression is defective in *cyd-1* mutants (this work). To ask if *cyd-1* and *fkh-6* function in the same regulatory pathway, we compared the effects of *fkh-6(0)* and *cyd-1(q626)* in double mutants with *tra-1*. It was previously seen that *fkh-6* has a synergistic effect with *tra-1*: the SGP lineages in *fkh-6; tra-1* double mutants arrest after one or, at most, two divisions (Chang et al., 2004). Similarly, we observed a synthetic phenotype in *cyd-1(q626); tra-1* double mutants (Figure 7A). This synthetic effect is less severe than that seen in *fkh-6; tra-1* double mutants, but the *cyd-1* mutant is not a null allele, and its effects on *fkh-6* gene expression are partially penetrant. The synthetic effect of both genes with *tra-1* supports the idea that *cyd-1* and *fkh-6* act in the same pathway.

We also examined *fkh-6(0); cyd-1(q626)* double mutants, and found no synergistic effect in males, as might be expected since *fkh-6* single mutants are fully penetrant (Figure 7A). By contrast, hermaphrodite gonads were affected more severely in *fkh-6(0); cyd-1(q626)* double mutants than in either single mutant (Figure 7A). It is important to note that the lack of gonadal arms in *fkh-6* single mutants results from a defect later in gonadogenesis than seen in *cyd-1* mutants (this work; Chang et al., 2004), and, furthermore, that POP-1 asymmetry was not affected in *fkh-6* mutants (see above). The simplest interpretation is that *cyd-1* and *fkh-6* control the generation of hermaphrodite gonadal arms by distinct mechanisms, and that the more severe phenotype typical of *fkh-6; cyd-1* double mutant hermaphrodites reflects an additive effect.

Discussion

Cyclin D Controls the SGP Asymmetric Division

Cyclin-dependent kinases (CDKs) and their cyclin binding partners are best known as regulators of the cell

cycle (Morgan, 1997). Of particular importance to this work is cyclin D, which has been implicated in the control of the G1/S transition (Sherr, 1994). In *C. elegans*, cyclin D and its CDK-4 partner promote the G1/S transition during most larval cell divisions (Boxem and van den Heuvel, 2001; Park and Krause, 1999). Cyclin D and CDK-4 counteract LIN-35/Rb, EFL-1/E2F, DPL-1/DP, and CKI-1, which, in turn, inhibit cyclin E and CDK-2 (Koreth and van den Heuvel, 2005). Therefore, the cell cycle machinery governing the G1/S transition has been conserved in *C. elegans*.

We have found that *cyd-1*, the single *C. elegans* cyclin D gene, controls the asymmetric division of the SGP, a highly regulated division that establishes organ axes and embarks on sex-specific programs of gonadogenesis (Kimble and Hirsh, 1979). Specifically, cyclin D affects both POP-1/TCF asymmetry and *fkh-6* expression in the early gonad. POP-1/TCF asymmetry is controlled by Wnt/MAPK signaling (Lo et al., 2004; Maduro et al., 2002), and, in the SGP daughters, it specifies gonadal axes (Siegfried et al., 2004). The FKH-6 transcription factor is a sex-determining gene that specifies the male gonadal fate (Chang et al., 2004). Therefore, *cyd-1* affects two key regulators of early gonadogenesis.

The *cyd-1* defects are specific for the SGP division. SGP divisions are delayed, but other larval blast cells divide normally; *fkh-6* and *rnr* expression are affected in SGPs, but other cells express these genes normally; and POP-1 asymmetry is abolished in the SGPs, but it occurs normally in non-gonadal blast cells. Why are the SGPs affected so specifically in *cyd-1(q626)* mutants? One possibility might have been that *cyd-1(q626)* identifies a domain that mediates an SGP-specific control. However, gonad defects typical of *cyd-1(q626)* mutants were also observed after *cyd-1* RNAi, which depletes cyclin D but does not eliminate it. We suggest that *cyd-1(q626)* is a partial loss-of-function allele, and that the SGP division is particularly sensitive to the level of cyclin D activity. Interestingly, the *cyd-1(cc600)* mutation also acts in a cell type-specific manner, affecting only the division of embryonically derived coelomocytes (Yanowitz and Fire, 2005). Therefore, individual cell divisions appear to have distinct requirements for *cyd-1* activity.

The SGP cell division is delayed in *cyd-1* mutants, raising the possibility that the cyclin D effects on POP-1 asymmetry and *fkh-6* expression might be nonspecific. Cell cycle length has been implicated as a factor in both cell fate specification and proper asymmetric divisions both in *C. elegans* and *Drosophila* (Ambros, 2001; Encalada et al., 2000; Fay, 2005; Fay and Han, 2000; Tio et al., 2001). However, delays of the SGP division by other methods did not mimic the *cyd-1* effect. Thus, hydroxyurea treatment, which slows S phase and delays cell divisions, had no apparent effect on gonadal development. Furthermore, *gon-4* RNAi, which delays the SGP division specifically (Friedman et al., 2000; this work), did not change the sex-specific asymmetry of the SGP division, POP-1 asymmetry, or *fkh-6* expression. Therefore, a simple delay in cell division is not likely to explain the cyclin D effects on the SGP asymmetric division.

Cyclin D Coordinates Regulators of SGP Asymmetric Division

We have found that cyclin D regulates three molecular markers in the SGPs or their daughters (Figure 7B). In the SGP itself, cyclin D affects expression of both *fkh-6::GFP* and *rnr::GFP*, a marker of S phase (Hong et al., 1998). Since *fkh-6* and *rnr* reporters are expressed with similar timing in the SGPs, an attractive idea is that *cyd-1* coordinates expression of both *fkh-6* and *rnr* as the cell progresses from G1 into S phase. In addition to its control of *fkh-6* and *rnr* in the SGPs, cyclin D affects POP-1 asymmetry in the SGP daughters. The linkage between the cyclin D control of POP-1 asymmetry and the G1/S transition is less evident. POP-1 asymmetry is first observed in SGP daughter cells soon after the SGP division (Siegfried et al., 2004; C.T., unpublished data). One possibility is that CYD-1 controls events in the SGP mother cell to subsequently affect POP-1 asymmetry in her daughters. If this is the case, we note that *fkh-6* is not required, because POP-1 asymmetry is not abolished in *fkh-6* null mutants. Alternatively, CYD-1 might influence POP-1 asymmetry in the daughters themselves. We attempted to distinguish between these two possibilities with temperature shifts, but the experiment did not have sufficient resolution (C.T., unpublished data). Regardless, the CYD-1 regulation of POP-1 and *fkh-6* appear to be distinct, suggesting that cyclin D is a common regulator of both gonadal regulators (Figure 7B).

Cyclin D Relieves E2F Repression to Promote *fkh-6* Expression

We have found that cyclin D works together with other major regulators of the G1/S transition to control the SGP asymmetric division (Figure 4). Most importantly, RNAi depletion of *efl-1*, which encodes an E2F-related transcription factor (Ceol and Horvitz, 2001), suppressed the *cyd-1* defects. This suppression was observed in both sexes, suggesting an effect of E2F on both POP-1 asymmetry and *fkh-6* expression. Although we do not know the specific Wnt/MAPK signaling component regulated, several lines of evidence suggest that *fkh-6* is controlled antagonistically by cyclin D and E2F: an *fkh-6* reporter was either not expressed at all in *cyd-1* mutant SGPs or expressed late; by contrast, *fkh-6* expression was restored in *cyd-1; efl-1(RNAi)* SGPs and was seen earlier than normal in *efl-1(RNAi)* SGPs. Therefore, cyclin D and E2F have opposite effects on *fkh-6* expression. Given the gonadal feminization by depletion of cyclin D, one might think a priori that depletion of E2F might masculinize the hermaphrodite gonad. However, in wild-type L1s, *fkh-6* is typically expressed in both hermaphrodite and male SGPs, and E2F depletion did not masculinize the hermaphrodite gonad. The simplest explanation is that E2F normally represses *fkh-6* expression, and that cyclin D relieves that repression. Although we identified a canonical E2F binding sequence in the *fkh-6* promoter, biochemical experiments will be required to learn whether *fkh-6* is a direct target of E2F repression. We conclude that the G1/S regulatory machinery controls *fkh-6* expression.

Cyclin D as a Key Regulator of Metazoan Development

Cyclin D is not an essential regulator of all metazoan cell cycles, a conclusion based on RNAi, deletion, and nonsense mutants of the single cyclin D gene in *C. elegans* (Boxem and van den Heuvel, 2001; Park and Krause, 1999); on deletion mutants of the single cyclin D gene in *Drosophila* (Emmerich et al., 2004); and on a triple knockout of the three cyclin D genes in mice (Kozar et al., 2004). Instead, cyclin D appears to be essential for a variety of developmental functions: regulation of the G1/S transition in most larval cell divisions in *C. elegans* (Boxem and van den Heuvel, 2001; Park and Krause, 1999), control of cell growth and cell number in *Drosophila* (Datar et al., 2000; Emmerich et al., 2004; Meyer et al., 2002), and regulation of heart development and expansion of hematopoietic stem cells in mice (Kozar et al., 2004). A caveat to interpreting these deletion studies is that other cyclins may fill in for cyclin D, an idea supported by genetic interactions with CDK-2 in *Drosophila* (Emmerich et al., 2004). Therefore, the scope of biological functions mediated by cyclin D and the G1/S cell cycle machinery more generally are poorly understood in metazoans.

Over the past ten years, it has become clear that G1/S cell cycle regulators are intimately linked with controls of cell fate. An early example was myoD, which drives muscle myoblasts out of the cell cycle by induction of p21(Waf1/Cip) (Halevy et al., 1995). In addition, myoD and cyclin D1 physically interact with each other and antagonize each other's activities (Zhang et al., 1999). Furthermore, *Drosophila* cyclin D/CDK-4 binds and stabilizes STAT92E, a control critical for embryonic segmentation (Chen et al., 2003), and mammalian cyclin E/CDK2 binds and phosphorylates cytosolic β-catenin, leading to its rapid degradation during G1 (Park et al., 2004). An effect of G1/S regulators on asymmetric divisions has also been seen in *Drosophila* (Prokopenko and Chia, 2005). Most strikingly, cyclin E controls the asymmetric division of an NB6-4 neuronal precursor (Berger et al., 2005). However, other components of the cell cycle machinery were not involved in this asymmetric division, and, therefore, this *Drosophila* control may be distinct from that reported here. While these previous results have forged a link between the cell cycle machinery and controls of cell fate, our findings extend this idea and suggest that cyclin D and other regulators of the G1/S transition coordinate the activity of multiple cell fate determinants during a single asymmetric cell division.

Experimental Procedures

Strains and Genetics

Standard protocols were used for culturing *C. elegans* strains (Sulston and Hodgkin, 1988). Strains were derived from the Bristol strain N2 and maintained at 20°C unless otherwise noted (Sulston and Horvitz, 1977). The high incidence of male mutation, *him-5(e1490)*, was included in strains to generate males (Hodgkin, 1983). The following mutations were used for this work: *LGI*, *lin-35(n745)*; *pop-1(q645)*; *sys-1(q736)*; *LGII*, *fkh-6(q641)*; *cyd-1(he116)*; *cyd-1(he112)*; *unc-52(e444)*; *dpy-10(e128)*; *unc-4(e120)*; *rol-1(e91)*; *bli-1(e769)*; *LGIII*, *tra-1(e1099)*; *LGIV*, *gon-4(q518)*; *LGV*, *him-5(e1490)*. The following integrated transgenes were used: *arIs51 [cdh-3::GFP]* (Pettitt et al., 1996); *ezIs1 [K09C8.2::GFP]* and *ezIs2 [fkh-6::GFP]* (Chang et al., 2004); *tnIs6 [lim-7::GFP]* (Hall et al., 1999); *maIs103 [rnr::GFP]* (Hong et al., 1998); *qIs74 [GFP::POP-1]* (Siegfried et al., 2004); *qIs76 [tra-1::GFP]* (Mathies et al., 2004); *qIs56 [lag-2::GFP]* (Blelloch et al., 1999); *qIs61 [pes-1::GFP]* (Molin et al., 2000); and *qIs77 [unc-122::GFP]* (Mathies et al., 2003). Extrachromosomal arrays used include: *leEx780 [ZK813.3::GFP, pRF4]* (a gift of Ian Hope); *qEx500 [hs::sys-1]* (Kidd et al., 2005). Balancers used include: *LGI* and *LGIII*, *hT2[qIs48]; LGII, mIn1[mIs14 dpy-10(e128)]; LG IV* and *V, nT1[qIs51]*. *qIs48* and *mIs14* carry the integrated array of *ccEx9747*, which is an extrachromosomal array of three GFP constructs: the *myo-2* and *pes-10* promoters and one driven by a gut-specific enhancer (Edgley and Riddle, 2001).

Isolation, Mapping, and Molecular Analysis of *cyd-1(q626)*

cyd-1(q626) was isolated in an F2 mutagenesis screen of *him-5(e1490)* animals for gonadogenesis defects. The *q626* mutation was then mapped to a region on *LGII* between *ptr-18* and *zyx-1* by using a combination of three-factor mapping and SNP mapping as described by Wicks et al. (2001). For SNP mapping, *q626*, non-*unc-52(e444)* mutant males were isolated, and the following primer sets were used to narrow the *q626* region: corresponding to C50E10: 22022, 5′-TCGGGTCTCTCCAAAAACTC-3′ and 3′-CTCCTTCAGTA CCATATGGCTC-5′, cut with EcoRI; corresponding to Y38F1A: 41752, 5′-TAGGAAAGTTGTGTCCACCTGG-3′ and 3′-TGATGACTC CTTCTTCAGCTGC-5′, cut with BamII; corresponding to F15D4: 22810, 5′-TTCCCATTTTCCTCCCAG-3′ and 3′-TCAAAAACCCAGA CACTGG-5′, cut with DraI; corresponding to F37B1:13109, 5′-TCT CCAAGATGAGAGAGAACCACTG-3′ and 3′-TCGCCGATTTGCTGG TACAG-5′, cut with AseI; corresponding to C31C9:11976, 5′-CAGTGACTAACGCCCCAAAACTC-3′ and 3′-GCTTCGTGTGATTCT TCTTTTGGG-5′, cut with NlaIII; corresponding to Y51H1A:30057, 5′-GATTCGGAATGGGTGTTG-3′ and 3′-TCTTGAATGCGTGGTGTG-5′, cut with TaqI; corresponding to Y48B6A:98880, 5′-GGTTTCCAGG TGATTCATAGCG-3′ and 3′-TATAGGACGGTTCGGTGAGAAG-5′, cut with NlaIII. *q626* was placed to the right of the SNP on Y38F1A and to the left of the SNP on F15D4. *q626* failed to complement two null alleles of *cyd-1*, *he112*, and *he116*. A PCR fragment containing 1000 bp upstream of the predicted start codon through the predicted poly(A) signal rescued *cyd-1(q626)* mutants. *cyd-1* RNAi was performed as described below. A template for sequencing of *cyd-1(q626)* was made by amplifying genomic DNA from N2 or *cyd-1(q626)* animals by using Roche PCR reagents. Three independent PCR reactions were sequenced for each *cyd-1* fragment amplified by using Big-Dye Terminator Ready Reaction Mix (PE/Applied Biosystems). Sequencing of *q626* DNA identified an A-to-G change in the third exon of the coding region.

DAPI Staining, Lineage Analysis, and Imaging

DAPI staining was performed as previously described by Kadyk and Kimble (1998). Briefly, animals were collected from plates in Eppendorf tubes and washed once in M9, fixed 5 min in −20°C methanol, washed twice in M9, stained with 0.1 μg/ml DAPI in M9 for 20 min, washed twice in M9, and mounted for fluorescence microscopy. Fluorescent images were captured with a Zeiss Axioskop by using Openlab software and were processed with Adobe Photoshop and Illustrator. Lineage analysis was performed by following cell divisions with standard DIC microscopy methods on a Zeiss Axioskop (Sulston and Horvitz, 1977). Males were identified by the presence of the large B blast cell in the tail.

RNAi and Hydroxyurea Experiments

All RNAi experiments were performed by growing synchronized larvae on bacteria expressing dsRNA as previously described (Ashrafi et al., 2003; Kamath et al., 2001), with the exception of RNAi corresponding to *cki-1/cki-2*, which was injected. For hydroxyurea treatment (HU), synchronized larvae were grown at 20°C for 6 hr, then transferred to plates containing 40 mM HU for 4–6 hr (Ambros, 1999). Larvae were then transferred back to normal plates. SGP cell division was assayed at the time larvae were transferred back to normal plates and at 1 hr intervals until division was observed. In all *gon-4(RNAi)* experiments, SGPs were delayed by approximately 3 hr compared to wild-type controls.

Acknowledgments

We gratefully acknowledge Victor Ambros, Ian Hope, Laura Mathies, Jonathan Pettitt, and Dave Zarkower for sharing GFP reporter strains, and members of the Kimble laboratory for discussions during the course of this work. We thank Anne Helsley-Marchbanks and Laura Vanderploeg for help preparing the manuscript and figures. J.K. is an investigator with the Howard Hughes Medical Institute (HHMI). C.T. was supported by a National Institutes of Health postdoctoral fellowship (F32 GM069716).

Received: May 31, 2005
Revised: August 15, 2005
Accepted: September 7, 2005
Published: October 3, 2005

References

Ahringer, J. (2003). Control of cell polarity and mitotic spindle positioning in animal cells. Curr. Opin. Cell Biol. *15*, 73–81.

Ambros, V. (1999). Cell cycle-dependent sequencing of cell fate decisions in *Caenorhabditis elegans* vulva precursor cells. Development *126*, 1947–1956.

Ambros, V. (2001). The temporal control of cell cycle and cell fate in *Caenorhabditis elegans*. Novartis Found. Symp. *237*, 203–214.

Ashrafi, K., Chang, F., Watts, J.L., Fraser, A.G., Kamath, R.S., Ahringer, J., and Ruvkun, G. (2003). Genome-wide RNAi analysis of *Caenorhabditis elegans* fat regulatory cells. Nature *421*, 268–272.

Bei, Y., Hogan, J., Berkowitz, L.A., Soto, M., Rocheleau, C.E., Pang, K.M., Collins, J., and Mello, C.C. (2002). SRC-1 and Wnt signaling act together to specify endoderm and to control cleavage orientation in early *C. elegans* embryos. Dev. Cell *3*, 113–125.

Berger, C., Pallavi, S.K., Prasad, M., Shashidhara, L.S., and Technau, G.M. (2005). A critical role for Cyclin E in cell fate determination in the central nervous system of *Drosophila melanogaster*. Nat. Cell Biol. *7*, 56–62.

Betschinger, J., and Knoblich, J.A. (2004). Dare to be different: asymmetric cell division in *Drosophila, C. elegans* and vertebrates. Curr. Biol. *14*, R674–R685.

Blelloch, R., Santa Anna-Arriola, S., Gao, D., Li, Y., Hodgkin, J., and Kimble, J. (1999). The *gon-1* gene is required for gonadal morphogenesis in *Caenorhabditis elegans*. Dev. Biol. *216*, 382–393.

Boxem, M., and van den Heuvel, S. (2001). *lin-35* Rb and *cki-1* Cip/Kip cooperate in developmental regulation of G1 progression in *C. elegans*. Development *128*, 4349–4359.

Ceol, C.J., and Horvitz, H.R. (2001). *dpl-1* DP and *efl-1* E2F act with *lin-35* Rb to antagonize Ras signaling in *C. elegans* vulval development. Mol. Cell *7*, 461–473.

Chang, W., Tilmann, C., Thoemke, K., Markussen, F.-H., Mathies, L.D., Kimble, J., and Zarkower, D. (2004). A forkhead protein controls sexual identity of the *C. elegans* male somatic gonad. Development *131*, 1425–1436.

Chen, X., Oh, S.-W., Zheng, Z., Chen, H.-W., Shin, H.-h., and Hou, S.X. (2003). Cyclin D-Cdk4 and cyclin E-Cdk2 regulate the Jak/STAT signal transduction pathway in *Drosophila*. Dev. Cell *4*, 179–190.

Coffman, J.A. (2004). Cell cycle development. Dev. Cell *6*, 321–327.

Cowan, C.R., and Hyman, A.A. (2004). Asymmetric cell division in *C. elegans*: cortical polarity and spindle positioning. Annu. Rev. Cell Dev. Biol. *20*, 427–453.

Datar, S.A., Jacobs, H.W., de la Cruz, A.F., Lehner, C.F., and Edgar, B.A. (2000). The *Drosophila* cyclin D-Cdk4 complex promotes cellular growth. EMBO J. *19*, 4543–4554.

Doe, C.Q., and Bowerman, B. (2001). Asymmetric cell division: fly neuroblast meets worm zygote. Curr. Opin. Cell Biol. *13*, 68–75.

Edgley, M.L., and Riddle, D.L. (2001). LG II balancer chromosomes in *Caenorhabditis elegans*: *mT1(II;III)* and the *mIn1* set of dominantly and recessively marked inversions. Mol. Genet. Genomics *266*, 385–395.

Emmerich, J., Meyer, C.A., de la Cruz, A.F., Edgar, B.A., and Lehner, C.F. (2004). Cyclin D does not provide essential Cdk4-independent functions in *Drosophila*. Genetics *168*, 867–875.

Encalada, S.E., Martin, P.R., Phillips, J.B., Lyczak, R., Hamill, D.R., Swan, K.A., and Bowerman, B. (2000). DNA replication defects delay cell division and disrupt cell polarity in early *Caenorhabditis elegans* embryos. Dev. Biol. *228*, 225–238.

Fay, D.S. (2005). The cell cycle and development: lessons from *C. elegans*. Semin. Cell Dev. Biol. *16*, 397–406.

Fay, D.S., and Han, M. (2000). Mutations in *cye-1*, a *Caenorhabditis elegans* cyclin E homolog, reveal coordination between cell-cycle control and vulval development. Development *127*, 4049–4060.

Friedman, L., Santa Anna-Arriola, S., Hodgkin, J., and Kimble, J. (2000). *gon-4*, a cell lineage regulator required for gonadogenesis in *Caenorhabditis elegans*. Dev. Biol. *228*, 350–362.

Halevy, O., Novitch, B.G., Spicer, D.B., Skapek, S.X., Rhee, J., Hannon, G.J., Beach, D., and Lassar, A.B. (1995). Correlation of terminal cell cycle arrest of skeletal muscle with induction of p21 by MyoD. Science *267*, 1018–1021.

Hall, D.H., Winfrey, V.P., Blaeuer, G., Hoffman, L.H., Furuta, T., Rose, K.L., Hobert, O., and Greenstein, D. (1999). Ultrastructural features of the adult hermaphrodite gonad of *Caenorhabditis elegans*: Relations between the germ line and soma. Dev. Biol. *212*, 101–123.

Herman, M.A. (2002). Control of cell polarity by noncanonical Wnt signaling in *C. elegans*. Semin. Cell Dev. Biol. *13*, 233–241.

Herman, M.A., and Horvitz, H.R. (1994). The *Caenorhabditis elegans* gene *lin-44* controls the polarity of asymmetric cell divisions. Development *120*, 1035–1047.

Hodgkin, J. (1983). Male phenotypes and mating efficiency in *Caenorhabditis elegans*. Genetics *103*, 43–64.

Hodgkin, J.A., and Brenner, S. (1977). Mutations causing transformation of sexual phenotype in the nematode *Caenorhabditis elegans*. Genetics *86*, 275–287.

Hong, Y., Roy, R., and Ambros, V. (1998). Developmental regulation of a cyclin-dependent kinase inhibitor controls postembryonic cell cycle progression in *Caenorhabditis elegans*. Development *125*, 3585–3597.

Hope, I.A. (1991). 'Promoter trapping' in *Caenorhabditis elegans*. Development *113*, 399–408.

Kadyk, L.C., and Kimble, J. (1998). Genetic regulation of entry into meiosis in *Caenorhabditis elegans*. Development *125*, 1803–1813.

Kamath, R.S., Martinez-Campos, M., Zipperlen, P., Fraser, A.G., and Ahringer, J. (2001). Effectiveness of specific RNA-mediated interference through ingested double-stranded RNA in *Caenorhabditis elegans*. Genome Biol. *2*, Research0002.0001–0002.0010.

Kidd, A.R., III, Miskowski, J.A., Siegfried, K.R., Sawa, H., and Kimble, J. (2005). A β-catenin identified by functional rather than sequence criteria and its role in Wnt/MAPK signaling. Cell *121*, 761–772.

Kimble, J. (1981). Alterations in cell lineage following laser ablation of cells in the somatic gonad of *Caenorhabditis elegans*. Dev. Biol. *87*, 286–300.

Kimble, J., and Hirsh, D. (1979). The postembryonic cell lineages of the hermaphrodite and male gonads in *Caenorhabditis elegans*. Dev. Biol. *70*, 396–417.

Kimble, J.E., and White, J.G. (1981). On the control of germ cell development in *Caenorhabditis elegans*. Dev. Biol. *81*, 208–219.

Koreth, J., and van den Heuvel, S. (2005). Cell-cycle control in *Caenorhabditis elegans*: how the worm moves from G1 to S. Oncogene *24*, 2756–2764.

Kozar, K., Ciemerych, M.A., Rebel, V.I., Shigematsu, H., Zagozdzon, A., Sicinska, E., Geng, Y., Yu, Q., Bhattacharya, S., Bronson, R.T., et al. (2004). Mouse development and cell proliferation in the absence of D-cyclins. Cell *118*, 477–491.

Lin, R., Thompson, S., and Priess, J.R. (1995). *pop-1* encodes an HMG box protein required for the specification of a mesoderm precursor in early *C. elegans* embryos. Cell *83*, 599–609.

Lo, M.-C., Gay, F., Odom, R., Shi, Y., and Lin, R. (2004). Phosphory-

lation by the β-catenin/MAPK complex promotes 14-3-3-mediated nuclear export of TCF/POP-1 in signal-responsive cells in *C. elegans*. Cell *117*, 95–106.

Maduro, M.F., Lin, R., and Rothman, J.H. (2002). Dynamics of a developmental switch: recursive intracellular and intranuclear redistribution of *Caenorhabditis elegans* POP-1 parallels Wnt-inhibited transcriptional repression. Dev. Biol. *248*, 128–142.

Mathies, L.D., Henderson, S.T., and Kimble, J. (2003). The *C. elegans* Hand gene controls embryogenesis and early gonadogenesis. Development *130*, 2881–2892.

Mathies, L.D., Schvarzstein, M., Morphy, K.M., Blelloch, R., Spence, A.M., and Kimble, J. (2004). *TRA-1/GLI* controls development of somatic gonadal precursors in *C. elegans*. Development *131*, 4333–4343.

Meyer, C.A., Jacobs, H.W., and Lehner, C.F. (2002). Cyclin D-Cdk4 is not a master regulator of cell multiplication in *Drosophila* embryos. Curr. Biol. *12*, 661–666.

Miskowski, J., Li, Y., and Kimble, J. (2001). The *sys-1* gene and sexual dimorphism during gonadogenesis in *Caenorhabditis elegans*. Dev. Biol. *230*, 61–73.

Molin, L., Mounsey, A., Aslam, S., Bauer, P., Young, J., James, M., Sharma-Oates, A., and Hope, I.A. (2000). Evolutionary conservation of redundancy between a diverged pair of forkhead transcription factor homologues. Development *127*, 4825–4835.

Morgan, D.O. (1997). Cyclin-dependent kinases: engines, clocks, and microprocessors. Annu. Rev. Cell Dev. Biol. *13*, 261–291.

Park, M., and Krause, M.W. (1999). Regulation of postembryonic G_1 cell cycle progression in *Caenorhabditis elegans* by a cyclin D/CDK-like complex. Development *126*, 4849–4860.

Park, C.S., Kim, S.I., Lee, M.S., Youn, C.-y., Kim, D.J., Jho, E.-h., and Song, W.K. (2004). Modulation of β-catenin phosphorylation/degradation by cyclin-dependent kinase 2. J. Biol. Chem. *279*, 19592–19599.

Pettitt, J., Wood, W.B., and Plasterk, R.H.A. (1996). *cdh-3*, a gene encoding a member of the cadherin superfamily, functions in epithelial cell morphogenesis in *Caenorhabditis elegans*. Development *122*, 4149–4157.

Prokopenko, S.N., and Chia, W. (2005). When timing is everything: role of cell cycle regulation in asymmetric division. Semin. Cell Dev. Biol. *16*, 423–437.

Roegiers, F., and Jan, Y.N. (2004). Asymmetric cell division. Curr. Opin. Cell Biol. *16*, 195–205.

Sherr, C.J. (1994). G_1 phase progression: cycling on cue. Cell *79*, 551–555.

Siegfried, K., and Kimble, J. (2002). POP-1 controls axis formation during early gonadogenesis in *C. elegans*. Development *129*, 443–453.

Siegfried, K.R., Kidd, A.R., III, Chesney, M.A., and Kimble, J. (2004). The *sys-1* and *sys-3* genes cooperate with Wnt signaling to establish the proximal-distal axis of the *C. elegans* gonad. Genetics *166*, 171–186.

Sternberg, P.W., and Horvitz, H.R. (1988). *lin-17* mutations of *Caenorhabditis elegans* disrupt certain asymmetric cell divisions. Dev. Biol. *130*, 67–73.

Sulston, J., and Hodgkin, J. (1988). Methods. In The nematode *Caenorhabditis elegans*, W.B. Wood, ed. (Cold Spring Harbor, NY: Cold Spring Harbor Laboratory Press), pp. 587–606.

Sulston, J.E., and Horvitz, H.R. (1977). Post-embryonic cell lineages of the nematode, *Caenorhabditis elegans*. Dev. Biol. *56*, 110–156.

Sulston, J.E., Schierenberg, E., White, J.G., and Thomson, J.N. (1983). The embryonic cell lineage of the nematode *Caenorhabditis elegans*. Dev. Biol. *100*, 64–119.

Tio, M., Udolph, G., Yang, X., and Chia, W. (2001). *cdc2* links the *Drosophila* cell cycle and asymmetric division machineries. Nature *409*, 1063–1067.

Wicks, S.R., Yeh, R.T., Gish, W.R., Waterston, R.H., and Plasterk, R.H.A. (2001). Rapid gene mapping in *Caenorhabditis elegans* using a high density polymorphism map. Nat. Genet. *28*, 160–164.

Yanowitz, J., and Fire, A. (2005). Cyclin D involvement demarcates a late transition in *C. elegans* embryogenesis. Dev. Biol. *279*, 244–251.

Zarkower, D., and Hodgkin, J. (1992). Molecular analysis of the *C. elegans* sex-determining gene *tra-1*: a gene encoding two zinc finger proteins. Cell *70*, 237–249.

Zhang, J.M., Chen, L., Krause, M., Fire, A., and Paterson, B.M. (1999). Evolutionary conservation of MyoD function and differential utilization of E proteins. Dev. Biol. *208*, 465–472.